

Online Neural Model Fine-Tuning in Massive MIMO CSI Feedback: Taming The Communication Cost of Model Updates

Mehdi Sattari, *Graduate Student Member, IEEE*, Deniz Gündüz, *Fellow, IEEE*, and
Tommy Svensson, *Senior Member, IEEE*

Abstract—Efficient channel state information (CSI) compression is essential in frequency division duplexing (FDD) massive multiple-input multiple-output (MIMO) systems due to the significant feedback overhead. Recently, deep learning-based compression techniques have demonstrated superior performance across various data types, including CSI. However, these methods often suffer from performance degradation when the data distribution shifts, primarily due to limited generalization capabilities. To address this challenge, we propose an online model fine-tuning approach for CSI feedback in massive MIMO systems. We consider full-model fine-tuning, where both the encoder and decoder are jointly updated using recent CSI samples. A key challenge in this setup is the transmission of updated decoder parameters, which introduces additional feedback overhead. To mitigate this bottleneck, we incorporate the bit-rate of model updates into the fine-tuning objective and entropy code the updates jointly with the compressed CSI. To reduce the bit-rate, we design an efficient prior distribution that encourages the network to update only the most significant weights, thereby minimizing the overall model update cost. Our results show that full-model fine-tuning significantly enhances the rate-distortion (RD) performance of neural CSI compression despite the additional communication cost of model updates. Moreover, we investigate the impact of update frequency in dynamic wireless environments and identify an optimal fine-tuning interval that achieves the best RD trade-off.

Index Terms—CSI compression, massive MIMO, deep learning, fine-tuning.

I. INTRODUCTION

MASSIVE multiple-input multiple-output (MIMO) is one of the key enabling technologies for 5G and beyond. By equipping the base station (BS) with massive antenna arrays, a large number of users can be served simultaneously through high-resolution beamforming techniques, resulting

M. Sattari, and T. Svensson are with the Department of Electrical Engineering, Chalmers University of Technology, Gothenburg, Sweden. E-mail: {mehdi.sattari, tommy.svensson}@chalmers.se. D. Gündüz is with the Department of Electrical and Electronic Engineering, Imperial College London, London, UK. E-mail: d.gunduz@imperial.ac.uk.

This work has been supported in part by the project SEMANTIC, funded by the EU's Horizon 2020 research and innovation programme under the Marie Skłodowska-Curie grant agreement No 861165, and in part by the Hexa-X-II project which has received funding from the Smart Networks and Services Joint Undertaking (SNS JU) under the European Union's Horizon Europe research and innovation programme under Grant Agreement No 101095759. D. Gündüz received funding from the UKRI through ERC consolidator project AI-R under grant EP/X030806/1, and from the Horizon Europe SNS project '6G-GOALS' under grant 101139232. The computations were enabled by resources provided by the National Academic Infrastructure for Supercomputing in Sweden (NAISS), partially funded by the Swedish Research Council through grant agreement no. 2022-06725.

in remarkable spectral efficiency. To enable massive MIMO technology, channel state information (CSI) must be available at both the BS and user sides. Various channel estimation techniques can be employed to estimate CSI by observing pilot signals. In time-division duplexing (TDD), only down-link/uplink channels need to be estimated, as the other channel can be derived thanks to reciprocity. However, in frequency-division duplexing (FDD), reciprocity does not hold, so the channels in both directions need to be estimated and fed back [1], [2].

To enable FDD transmission for massive MIMO systems, CSI compression techniques are critical to circumvent excessive feedback overhead. Various CSI compression techniques have been studied in the literature by employing compressed sensing [3], [4], vector quantization [5], [6], and more recently deep learning tools [7]–[15]. Due to strong spatial correlation, the CSI matrix can exhibit sparsity in certain domains, and compressed sensing methodologies can be applied to efficiently compress the large CSI matrix [3], [4]. However, these algorithms often struggle to find the best basis to project the CSI matrix to lower dimensions. Furthermore, compressed sensing-based algorithms are iterative and time-consuming, making them infeasible for deployment in massive MIMO channels. Similarly, in vector quantization for CSI compression [5], [6], the overhead scales linearly with the channel dimension, rendering it impractical for massive MIMO systems.

Recent advances in data-driven compression approaches, driven by the progress in neural network (NN) architectures have gained substantial interest in all data modalities [16]. Neural data compression is a machine learning technique that performs the compression task using deep neural networks (DNNs). Current research in neural compression is largely driven by the development of deep generative models such as generative adversarial networks (GANs) [17], variational autoencoders (VAEs) [18], normalizing flows [19], and autoregressive models [20] for image and video compression. These models have proven effective in capturing complex data distributions, which is crucial for achieving high compression rates while maintaining data fidelity.

In the wireless communication domain, the first neural CSI compressor was introduced in [7], where the authors used a simple convolutional neural network (CNN) auto-encoder architecture for dimension reduction of a massive MIMO channel matrix. Later, numerous network architec-

tures and machine learning techniques have been proposed to further improve the CSI compression efficiency [8]–[11]. While most works formulated the problem in terms of the dimensions of the reduced CSI matrix, the feedback channels must ultimately convey the CSI matrix in bits, necessitating additional quantization in the latent space. In [14] and [21], the authors formulated the problem within the rate-distortion (RD) framework and further enhanced the performance of the neural CSI compressor by incorporating learned entropy encoding and decoding blocks. They employed a weighted RD loss function to jointly minimize the mean squared error (MSE) and the average bit-rate overhead, explicitly quantifying the communication cost of compression in bits per CSI dimension under a variable-rate compression scheme.

Machine learning models often perform remarkably well on test sets with a distribution similar to their training data but can fail catastrophically in deployment when the data distribution shifts. Such shifts can arise from various factors, including temporal changes, domain variations, or sampling biases, and pose significant challenges in many real-world applications [22]. Several approaches, such as transfer learning [23], data augmentation [24], and domain adaptation [25], can be employed to enhance the robustness of machine learning models against distribution shift and improve their generalization capabilities. In transfer learning, models trained on generic datasets are fine-tuned for the target domain. Data augmentation improves generalization by artificially generating diverse training samples. Domain adaptation, on the other hand, aligns source and target domain distributions through techniques such as instance re-weighting or feature alignment.

Distribution shift is a common phenomenon in wireless networks. The statistics of the underlying wireless channel change due to various factors such as user mobility, environmental changes, or variations in interference from other devices. When the channel distribution deviates from initial assumptions or models, the efficiency of algorithms for tasks such as channel estimation [26], signal detection [27], etc can degrade. Consequently, maintaining robust communication requires adaptive strategies that can adjust to these shifts. In the context of CSI compression for FDD massive MIMO systems, most models in the literature are trained and tested using data from the same environment, e.g., within a specific macro-cell coverage area. However, this would require users to either store or download [28] new models for every new cell they enter, making these approaches infeasible in practice. Therefore, it is crucial to develop techniques that can overcome the distribution shift problem in CSI compression.

Several works have studied the effect of distribution shift in the CSI compression problem [29]–[35]. In [29], a deep transfer learning method is used to handle the distribution shift and reduce training costs. Additionally, a model-agnostic meta-learning algorithm is proposed to reduce the number of CSI samples needed for fine-tuning the pre-trained model. A lightweight translation model and data augmentation method based on domain knowledge are introduced in [30]. Specifically, to adapt to new channel conditions, the authors propose an efficient scenario-adaptive CSI feedback architecture, “CSI-TransNet,” and an efficient deep unfolding-based CSI

compression network, “SPTM2-ISTANet+.” A single-encoder-to-multiple-decoders (S-to-M) approach is presented in [31], where the authors use multi-task learning to integrate multiple independent autoencoders into a unified architecture featuring a shared encoder and several task-specific decoders.

The authors in [32] proposed an online learning scheme using a vanilla autoencoder network and considered different schemes, including encoder-only, decoder-only, and full-model updates. Similarly, encoder-only and full-model online learning approaches are considered in [33], and elastic weight consolidation (EWC) is proposed to overcome the catastrophic forgetting problem in NNs. A federated edge learning (FEEL)-based training framework is introduced in [34] for massive MIMO CSI feedback, and different quantization resolutions are considered for model update transmission to reduce the communication overhead. In [35], encoder-only online learning is employed and extended to the multi-user scenario via gossip learning. Additionally, two data augmentation strategies, namely, random erasing and random phase shift (RPS), are introduced.

However, we highlight that the communication overhead associated with model updates is neglected in all the aforementioned prior works. This represents a significant gap in the literature, as typical DNNs can contain millions of parameters, and transmitting model updates can result in massive feedback overhead. The authors in [34] employ a low-resolution quantization scheme for model update transmission, such as 2-bit or 4-bit quantization, but ignore the model update bit-rate. To elaborate, the decoder network in [34] includes approximately 4 million trainable parameters. Even with an aggressive 2-bit quantization, the resulting communication overhead would be around 8 Mbits, substantially higher than that is required to transmit the compressed CSI matrix. More precisely, a compressed CSI matrix of size 64×64 , using a modest compression ratio of 16, would only require 4 kbits and 16 kbits for 2-bit and 32-bit quantization, respectively. Comparing the communication cost for compressed CSI and model updates illustrates that transmitting model updates can introduce a prohibitive feedback overhead for fine-tuning in FDD massive MIMO systems.

To bridge this gap, in this paper, we explicitly account for the communication overhead of model update transmission. We investigate how to efficiently transmit both the model updates and the latent compressed CSI to obtain the best overall RD trade-off. The key differences and contributions of this work are summarized as follows:

- Prior works tackling the distribution shift problem in CSI compression have only concentrated on vanilla autoencoder-based CSI compression, neglecting the bit-level CSI compression and model update transmission [29]–[35]. For the first time in the literature, we quantify the RD trade-off in CSI compression by taking into account the communication cost of both the compressed CSI and the model updates. By introducing lossless entropy coding schemes for latent compressed CSI as well as model updates, we show that the problem of communication overhead can be further optimized in online fine-tuning of CSI feedback.

- For efficient entropy coding of model updates, we apply a spike-and-slab prior to model the distribution of these updates. This prior comprises a mixture of narrow (spike) and wider (slab) Gaussian distributions. By assigning more weight to the spike component, the prior encourages the network to select only the most impactful parameters, thereby significantly improving the RD performance. Additionally, we include the bit rate of model updates as a regularizer in the RD loss function. Simulation results confirm that both the spike-and-slab prior and the regularization are crucial for minimizing the cost of model updates.
- We investigate how often fine-tuning should be applied to update the neural model. The less the model update frequency is, the smaller the bit-rate cost for model updates, but the higher the compression rate to achieve the same CSI distortion due to the mismatch between training and test statistics. On the other hand, a higher model update frequency would make CSI compression more efficient, but at the cost of increased bit-rate for model update feedback. Our analysis identifies an optimal update frequency resulting in the best RD trade-off.

The rest of this paper is organized as follows: Section II introduces the model for the FDD massive MIMO system as well as our low-complexity backbone neural CSI compressor. In Section III, we present the encoder-only and full-model fine-tuning algorithms. Section IV provides numerical simulations and compares different fine-tuning schemes in terms of the RD trade-off. Finally, Section V concludes the paper.

Throughout the paper, the following notations are used: Matrices are represented using bold uppercase letters, while bold lowercase letters denote vectors. The transpose is denoted by the superscript $(\cdot)^T$. We use \mathbb{E} to denote expectation and $\|\cdot\|$ to represent the norm. The symbols $\lfloor \cdot \rfloor$, $\lfloor \cdot \rfloor$, and $\lceil \cdot \rceil$ are used to define the round, floor, and ceil operations, respectively.

II. FDD MASSIVE MIMO AND BACKBONE NEURAL CSI COMPRESSOR

A. FDD Massive MIMO

We consider FDD transmission, where a massive MIMO BS serves several single-antenna users. The BS is equipped with a uniform planar array (UPA) of N_t antennas. Orthogonal frequency division multiplexing (OFDM) is used for downlink transmission across N_c subcarriers. For each subcarrier m , let $\mathbf{h}_m \in \mathbb{C}^{N_t}$ denote the channel vector from the BS to one of the users, $\mathbf{w}_m \in \mathbb{C}^{N_t}$ the transmit precoding vector, $x_m \in \mathbb{C}$ the transmitted data symbol, and $n_m \in \mathbb{C}$ the additive noise. The received signal at the user over that subcarrier is given by:

$$y_m = \mathbf{h}_m^T \mathbf{w}_m x_m + n_m. \quad (1)$$

The downlink CSI matrix in the spatial-frequency domain is denoted by:

$$\mathbf{H} = [\mathbf{h}_1, \dots, \mathbf{h}_{N_c}] \in \mathbb{C}^{N_t \times N_c}. \quad (2)$$

CSI is crucial for precoding the transmitted signal in downlink transmission and decoding the received uplink signal. In

FDD systems, the reciprocity between uplink and downlink channels does not hold, necessitating pilot signal transmission from both the user and the BS. After receiving these pilot signals, the downlink and uplink channels are estimated at the user and the BS, respectively. For downlink transmission, each user sends its estimated channel matrix back to the BS via a feedback link. In massive MIMO systems, the channel matrix is large, making it extremely expensive in terms of bandwidth to feedback the entire channel matrix. To address this bottleneck, CSI compression is typically employed. In this process, the CSI matrix is compressed by the user by mapping it to a codeword from a compression codebook. The BS then reconstructs the channel matrix in a lossy fashion. The goal of CSI compression in FDD massive MIMO systems is to minimize the reconstruction loss while adhering to a prescribed feedback bit-rate constraint from the user to the BS.

B. Backbone Neural CSI Compressor

While many prior works on CSI compression have focused on optimizing the distortion loss associated with feedbacking a low-dimensional representation of the CSI matrix, they often overlook optimizing the bit-rate required to transmit the compressed CSI matrix. An exception to this is the works in [14], [21]. Building on [14], [21], we prioritize optimizing the RD trade-off in CSI compression, rather than solely minimizing the distortion achieved through dimensionality reduction of the CSI matrix.

To this end, we incorporate quantization, entropy encoding, and entropy decoding to optimize the feedback rate during the training of a neural CSI compressor. Our neural CSI compressor, denoted by $c = (f_\phi, g_\theta, \gamma_\theta)$, comprises a feature encoder $f_\phi : \mathbb{C}^{N_t \times N_c} \rightarrow \mathcal{Z}$, parameterized by ϕ , a feature decoder $g_\theta : \mathcal{Z} \rightarrow \mathbb{C}^{N_t \times N_c}$ and an entropy code γ_θ , jointly parameterized by θ [16]. For simplicity, we use the same symbol (θ) for the parameter space of the feature decoder and the entropy code.

The *encoder* maps each CSI matrix $\mathbf{H} \in \mathbb{C}^{N_t \times N_c}$ to a latent representation $\mathbf{Z} \in \mathcal{Z}$. This latent representation is quantized into bits and transmitted losslessly to the receiver using a variable-length entropy code. Let $\bar{\mathbf{Z}} = Q(\mathbf{Z})$ denote the quantized latent representation, where $Q(\cdot)$ is the quantization operation. Entropy encoder converts the quantized latent values to a bit stream using a lossless coding scheme, $b_z = \gamma_\theta(\bar{\mathbf{Z}}; p_\theta)$, where p_θ is the prior probability modeling the distribution of the latent space.

At the *decoder*, entropy decoder is first applied to recover the quantized latent vector from the bit stream, $\mathbf{Z} = \gamma^{-1}(b_z; p_\theta)$; and the de-quantization function is applied to recover the continuous latent values, $\hat{\mathbf{Z}} = Q^{-1}(\mathbf{Z})$. We should stress that $Q^{-1}(\cdot)$ is not necessarily representing the inverse of $Q(\cdot)$ and this function is not bijective in lossy compression. Both the encoder and decoder utilize a shared entropy code γ_θ with a prior probability p_θ to ensure the lossless transmission of the quantized latent representation $\bar{\mathbf{Z}}$. The feature decoder reconstructs the decompressed CSI matrix

from the de-quantized latent representation $\hat{\mathbf{Z}}$, expressed as $\hat{\mathbf{H}} = g_\theta(\hat{\mathbf{Z}})$.

Let the distortion function be denoted as $\rho : \mathbf{H} \times \hat{\mathbf{H}} \rightarrow [0, \infty)$, representing the error between the ground truth CSI matrix and its corresponding reconstruction. Typically, this error is calculated as the squared error $\rho(\mathbf{H}, \hat{\mathbf{H}}) \propto \|\mathbf{H} - \hat{\mathbf{H}}\|^2$. In lossy compression, we can formalize the distortion as follows:

$$D(c) = \mathbb{E} [\rho(\mathbf{H}, \hat{\mathbf{H}})], \quad (3)$$

where the expectation is taken over the random realization of the channel matrix \mathbf{H} , as we can limit our attention to deterministic codes without loss of optimality [36]. If we define the bit length corresponding to the CSI matrix \mathbf{H} as $l(\mathbf{H}) := |\gamma_\theta(Q(f_\phi(\mathbf{H})))|$, then the average bit-rate can be defined as follows:

$$R(c) = \mathbb{E} [l(\mathbf{H})], \quad (4)$$

which, in principle, represents the number of bits required for encoding the CSI matrix \mathbf{H} . This average can be approximated by the entropy of the quantized values:

$$R(c) = \mathbb{E} [-\log_2 p_\theta(\bar{\mathbf{Z}})]. \quad (5)$$

The objective here is to jointly minimize the distortion and rate with respect to the encoder, decoder, and latent parameters. According to rate-distortion theory, the fundamental limits of lossy compression can be characterized through a conditional distribution $p_{\hat{\mathbf{H}}|\mathbf{H}}$. The RD function is then given by:

$$R(D) = \inf_{p_{\hat{\mathbf{H}}|\mathbf{H}}: \mathbb{E} [\rho(\mathbf{H}, \hat{\mathbf{H}})] \leq D} I[\mathbf{H}; \hat{\mathbf{H}}], \quad (6)$$

where $I[\mathbf{H}; \hat{\mathbf{H}}]$ is the mutual information between the CSI matrix \mathbf{H} and its reconstruction $\hat{\mathbf{H}}$. Theoretically, this optimal rate can be achieved using vector quantization but requires compressing many independent realizations of the channel matrix jointly. This approach is intractable with high-dimensional data; and moreover, in practice, we need to compress each CSI matrix individually. To circumvent this problem, an *operational rate-distortion trade-off* can be defined, where we denote the set of all acceptable codecs under consideration by \mathcal{C} :

$$R_O(D) = \inf_{c \in \mathcal{C}: \mathbb{E} [\rho(\mathbf{H}, \hat{\mathbf{H}})] \leq D} \mathbb{E} [l(\mathbf{H})], \quad (7)$$

which can be optimized by introducing the Lagrangian:

$$L(\lambda, c) = R(c) + \lambda D(c) = \mathbb{E} [l(\mathbf{H})] + \lambda \mathbb{E} [\rho(\mathbf{H}, \hat{\mathbf{H}})]. \quad (8)$$

For any λ , the minimum of the above objective over \mathcal{C} yields an optimal codec c^* . Here, λ acts as a regularizer that governs the trade-off between the rate and distortion terms. Larger values of λ push the neural CSI compressor toward the higher bit-rate region with a better distortion performance, and vice versa. By applying the MSE function for distortion, the RD loss is formulated in (9) at the bottom of this page.

Furthermore, it has been shown that the rate-distortion for lossy compression can be interpreted as a VAE [37], and an upper bound on the rate-distortion function is given by:

$$L_{RD}(\phi, \theta) = D_{KL}[q_\phi(z|x) || p_\theta(z)] + \lambda \mathbb{E}_{q_\phi(z|x)} [-\log p_\theta(x|z)], \quad (10)$$

where $q_\phi(z|x)$ is the encoder conditional distribution parameterized by ϕ , $p_\theta(x|z)$ is the decoder conditional distribution parameterized by θ , and $p_\theta(z)$ is the latent prior parameterized jointly with the decoder parameters by θ . $\mathbb{E}_{q_\phi(z|x)} [-\log p_\theta(x|z)]$ represents the expected log-likelihood of the data given the latent variable z . This can be seen as minimizing the distortion D , where distortion measures how well the reconstructed data matches the original data. The KL divergence term $D_{KL}[q_\phi(z|x) || p_\theta(z)]$ measures the divergence between the learned latent distribution $q_\phi(z|x)$ and the prior $p_\theta(z)$. This term acts as a regularizer, ensuring that the latent representation z does not deviate too much from the prior, which can be interpreted as controlling the rate R .

Fig. 1 depicts our encoder/decoder architectures, where the input consists of the real and imaginary parts of the spatial-frequency channel matrix. The encoder function f_ϕ comprises several convolutional layers with accompanying activation functions that transform the high-dimensional massive MIMO channel matrix \mathbf{H} into a lower-dimensional latent representation. Specifically, for the first two layers, we apply convolutional layers with 64 kernels and ReLU activation functions, while for the last layer, the number of convolutional kernels is 2, and a linear activation function is applied. Max pooling is used to reduce the dimension of the input spatial-frequency channel matrix. We explore two different CSI dimensions, 256×256 and 64×64 , throughout this paper.

After acquiring the low-dimensional latent space, quantization and entropy coding are applied to transform the latent representation into a bit sequence. Specifically, a uniform scalar quantizer with a unit quantization bin is used to convert continuous latent values into discrete values. Based on the latent probability distribution learned during training, a lossless compression algorithm such as range coding or context-adaptive binary arithmetic coding (CABAC) is utilized to entropy code the quantized latent space, resulting in a variable-length bit stream. Incorporating quantization into the compressor poses a challenge for training through backpropagation since the derivative of quantization is zero almost everywhere. To circumvent this problem, a common practice is to approximate the quantization by adding independent and identically distributed (i.i.d.) uniform noise, $\Delta \mathbf{Z} \sim U(0, 1)$, to the latent representation, i.e., $\tilde{\mathbf{Z}} = \mathbf{Z} + \Delta \mathbf{Z}$. This approach yields a differentiable upper bound on the number of bits needed to compress the latent space. During inference, a more accurate estimate of the number of compressed bits is obtained using the actual quantization output, i.e., without i.i.d. uniform noise.

$$L_{RD}(\phi, \theta) = \mathbb{E} [-\log_2 p_\theta(Q(f_\phi(\mathbf{H}))) + \lambda \|g_\theta(Q^{-1}(Q(f_\phi(\mathbf{H}))) - \mathbf{H}\|^2]. \quad (9)$$

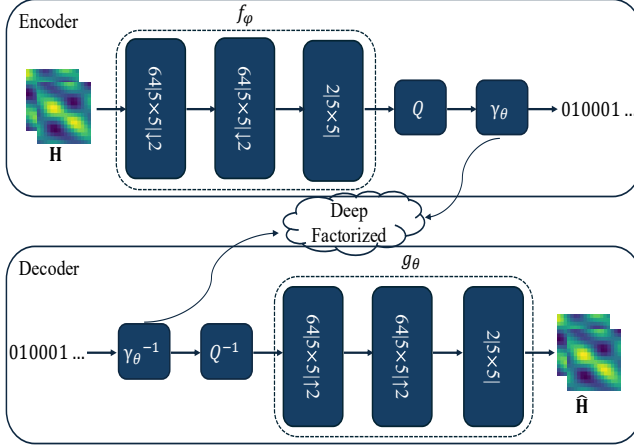


Fig. 1: The neural CSI compressor architecture.

On the decoder side, the entropy-coded quantized bit stream is first decoded, and the low-dimensional channel matrix is recovered by the decoding network. The entropy encoder and decoder share the same prior distribution for the latent variable. In our architecture, we adopt a fully factorized distribution based on a neural network cumulative called DeepFactorized [38]. This distribution leverages DNNs to learn and represent the latent distributions while assuming certain factorization properties. The decoder neural network, function g_θ in our model depicted in Fig. 1, consists of convolutional layers, each with a kernel size of 5. Similar to the encoder network, the ReLU activation function is used throughout. To reconstruct the large channel matrix from the low-dimensional entropy-decoded representation, an upsampling function is applied.

C. Experimental Evaluation of The Backbone Neural CSI Compressor

To assess the performance of the trained neural CSI compressor, we utilize the DeepMIMO dataset, which constructs the MIMO channels based on ray-tracing simulations from Remcom Wireless InSite [39]. Specifically, we train our neural CSI compressor in a static outdoor scenario referred as ‘O1’ at 28 GHz carrier frequency. More details about the parameter setup of this dataset in our simulations are provided in Table I. We generate 11,920 and 29,865 channel realizations, respectively, for 256×256 and 64×64 CSI dimensions and separate 40%, 40%, and 20% of these CSI samples as the training, validation, and test datasets, respectively. For training, we utilize the RD loss function defined in (9). In particular, the goal of training is to find optimal values for encoder and decoder weights together with the factorized distribution to be used in entropy coding. The backbone neural CSI compressor is trained on Python 3.9 and implemented using the TensorFlow libraries. We employ Adam optimizer with a learning rate of 0.001 and batch size of 32 to update the network parameters for 200 epochs.

We assess the performance of the neural CSI compressor in terms of the RD trade-off achieved, where the distortion

TABLE I: DeepMIMO dataset parameters

DeepMIMO parameters	Value
Scenario	O1
Center frequency	28 GHz
Number of paths	10
Active users	from row 1100 to 2200
Active BS number	BS 5
Bandwidth	50 MHz
Number of OFDM subcarriers	256 (64)
BS antennas	$N_x = 1, N_y = 64$ (64), $N_z = 4$ (1)
UE antennas	$N_x = 1, N_y = 1, N_z = 1$

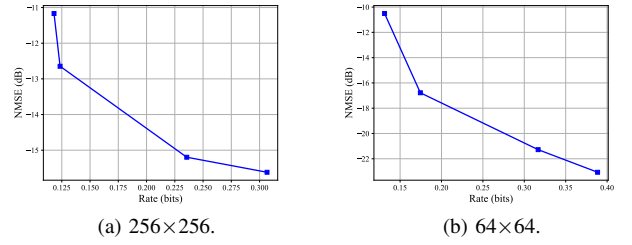


Fig. 2: RD performance of the backbone neural CSI compressor for different CSI dimensions.

is measured as the normalized mean squared error (NMSE), defined as

$$\text{NMSE} \triangleq \mathbb{E} \left[\frac{\|\mathbf{H} - \hat{\mathbf{H}}\|^2}{\|\mathbf{H}\|^2} \right], \quad (11)$$

where \mathbf{H} and $\hat{\mathbf{H}}$ are the true and reconstructed channel matrices, respectively. The bit-rate of the entropy-coded latent representation is estimated using (5).

The RD curve in Fig. 2 illustrates the performance of our trained neural CSI compressor across various values of λ . For the 256×256 CSI dimension, each point in the RD plot corresponds to $\lambda = 5 \times 10^5, 10^6, 5 \times 10^6$, and 10^7 , while for the 64×64 case, the RD weights for each point are $\lambda = 5 \times 10^4, 10^5, 5 \times 10^5$, and 10^6 . This figure confirms that the trained neural CSI compressor performs well when tested with (unseen) CSI realizations sampled from the same environment.

III. CSI FEEDBACK FINE-TUNING

One of the main challenges in using any learning methodologies, particularly in dynamic environments, is dealing with distribution shifts. A distribution shift occurs when the statistical properties of the data change between the training phase and the deployment phase. Due to limited model capacity or an insufficient amount of data, the performance of trained models can significantly drop, hindering their effectiveness in real-world applications. This phenomenon is particularly problematic in applications like neural CSI compression in wireless communication systems.

To analyze the effect of distribution shift, we test our trained model in a completely different environment. Specifically, we use two different datasets, QuaDRiGa [40] and DeepMIMO (in a different scenario), to evaluate the RD performance of our

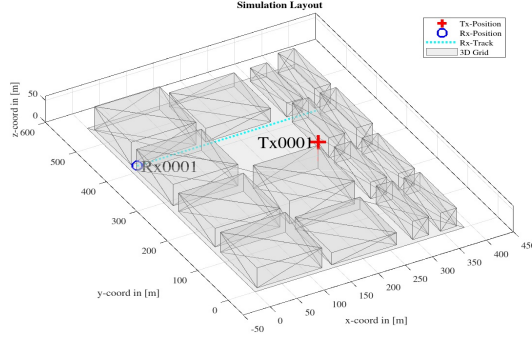


Fig. 3: Simulation layout of QuaDRiGa dataset [40].

TABLE II: QuaDRiGa dataset parameters

parameters	Value
Center frequency	3.7 GHz
Bandwidth	50 MHz
Number of OFDM subcarriers	256 (64)
Number of BS Antennas	256 (64)
Number of user Antennas	1
User (initial) position	(15, 415, 1.2)
BS position	(267, 267, 60)
BS orientation	$\pi/2$ (facing north)
Sample frequency	29.6 samples/meter

neural CSI compressor. In the QuaDRiGa channel generator, we setup a simulation with a BS equipped with a uniform planar array of 256 (64) antenna elements and 256 (64) OFDM subcarriers, simulating an urban deployment with the BS on a rooftop. The mobile user moves along a linear track of 350 meters at a speed of 5 km/h. The 3D model for this simulation is based on the Madrid grid developed by the METIS project. The simulation layout is shown in Fig. 3, and the parameters for this dataset are summarized in Table II.

For the DeepMIMO dataset, we use a dynamic scenario referred to as ‘O2 dynamic’. CSI realizations in this scenario are captured across different scenes at a sampling rate of 100 ms. The top view of this scenario is shown in Fig. 4, which features three streets and two intersections. Vehicles in the streets change positions in each scene, out of 1,000 captured scenes, and there are 2 BSs and 115,000 candidate users. The simulation setup details for this scenario are summarized in Table III.

To evaluate how well our neural CSI compressor performs in these new environments, we assess the RD performance in Fig. 5. The model is tested on the QuaDRiGa dataset in Fig. 5a and on the DeepMIMO ‘O2 dynamic’ dataset in Fig. 5b. As shown in these plots, our trained neural CSI compressor struggles with the new channel statistics and performs catastrophically. These results highlight the need for an effective fine-tuning strategy for the CSI compression problem in massive MIMO systems.

A trained model can be adapted to new channel statistics by exposing it to data samples from the new environment. Fine-tuning a neural CSI compressor involves updating the backbone model parameters, i.e., ϕ_0 and θ_0 for the encoder and decoder network, respectively, that was trained on a generic

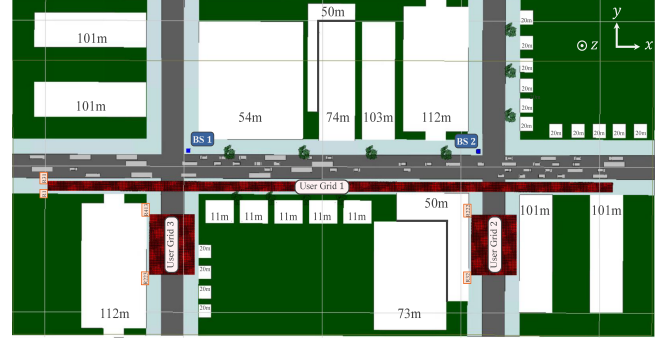


Fig. 4: The top view of the ‘O2 Dynamic’ scenario [41].

TABLE III: DeepMIMO dataset parameters

DeepMIMO parameters	Value
Scenario	O2 Dynamic
Center frequency	3.5 GHz
Number of paths	10
Active users	from row 1 to 31
Scene number	1
Active BS number	BS 1
Bandwidth	50 MHz
Number of OFDM subcarriers	256 (64)
BS antennas	$N_x = 1, N_y = 64, N_z = 4$ (1)
UE antennas	$N_x = 1, N_y = 1, N_z = 1$

dataset (the ‘O1 static’ DeepMIMO dataset in our simulations). Fine-tuning the backbone neural CSI compressor with new CSI samples (the ‘O2 static’ DeepMIMO and QuaDRiGa datasets in our simulations) results in updated parameters, ϕ and θ , for the encoder and decoder network, respectively, where only the decoder parameters need to be conveyed in the bitstream. To fine-tune our model, we first introduce an encoder-only fine-tuning scheme, followed by a focus on fine-tuning the entire model end-to-end.

A. Encoder-Only Fine-Tuning

Updating the decoder and latent parameters requires transmitting model updates to the decoder side. Therefore, one possible approach is to update only the encoder parameters while freezing the decoder and latent weights. This enables partial fine-tuning of the trained model without requiring additional feedback. Similar strategies have been explored in prior works, particularly using vanilla autoencoders with different network architectures [32], [33], [35]. The steps for encoder-only fine-tuning are summarized in Algorithms 1 and 2. It is important to emphasize that during fine-tuning and parameter updates, we use CSI samples collected in the new environment, denoted as \mathcal{H}_T . For evaluation, however, the fine-tuned network is applied to CSI samples collected after the fine-tuning period, denoted as \mathcal{H}_E . Fig. 6 shows how CSI samples are used for the fine-tuning and evaluation phase in our considered fine-tuning schemes.

Although encoder-only fine-tuning is attractive due to its simplicity, as the encoder can fine-tune its parameters locally with the available CSI samples, we show through simulations in Section IV that it results in only a marginal boost in the RD performance of the neural CSI compression.

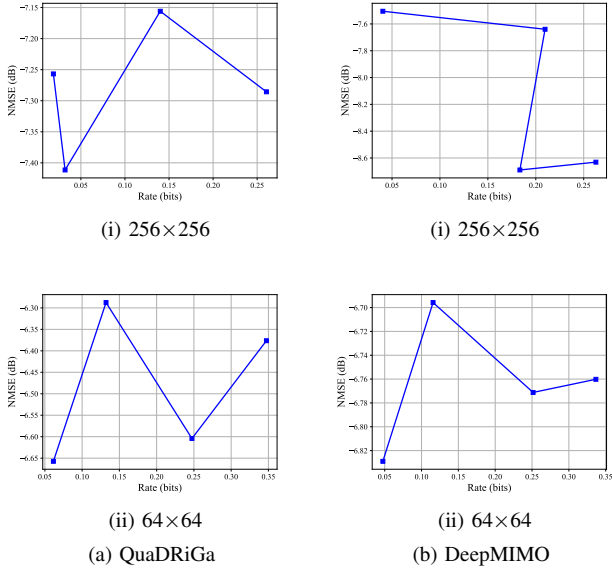


Fig. 5: RD plots for the backbone neural CSI compressor trained on the DeepMIMO ‘O1 static’ dataset and tested on (a) QuaDRiGa and (b) DeepMIMO ‘O2 dynamic’ CSI samples.

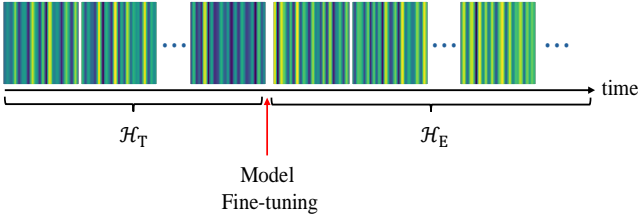


Fig. 6: CSI samples used for fine-tuning and evaluation. The fine-tuned neural CSI compressor is evaluated using CSI samples after the fine-tuning period.

B. Full-Model Fine-Tuning

In full-model fine-tuning, we aim to fine-tune the entire model; that is, both the encoder and decoder network, while accounting for the additional communication overhead for the decoder model updates that must be conveyed from the transmitter to the receiver. Specifically, we encode the decoder model updates $\delta \triangleq \theta - \theta_0$ alongside the latent space, i.e., z . To encode the decoder model update vector, we first need to quantize it. Unlike the unit bin quantization used for the latent space, we employ a higher-resolution quantization for model updates, as they vary only slightly depending on the learning rate. In particular, we use N equispaced bins of width t and define the quantization function for model updates as follows [42]:

$$\bar{\delta} = Q_t(\delta) = \text{clip} \left(\left\lfloor \frac{\delta}{t} \right\rfloor t, -\frac{(N-1)t}{2}, \frac{(N-1)t}{2} \right), \quad (12)$$

Algorithm 1 Encoder-only Fine-tuning - Encoder

Input: Global model parameters $\{\theta_0, \phi_0\}$ trained on a generic dataset, batch size B , CSI samples in the new environment $\mathcal{H} = \{\mathcal{H}_T, \mathcal{H}_E\}$.

Output: Compressed bitstream b_z .

Initialize model parameters: $\phi = \phi_0$, $\theta = \theta_0$.

for epoch = 1 to num_epochs **do**

for each batch b in \mathcal{H}_T **do**

 Load data batch $\mathbf{H} \in \{\mathcal{H}_b\}_{b=1}^B$ from \mathcal{H}_T .

 Apply feature encoder and quantization, $\mathbf{Z} = f_\phi(\mathbf{H})$ and $\tilde{\mathbf{Z}} = \mathbf{Z} + \Delta\mathbf{Z}$.

 Apply feature decoder, $\hat{\mathbf{H}} = g_\theta(\tilde{\mathbf{Z}})$.

 Compute RD loss $L_{\text{RD}}(\phi, \theta)$ according to equation (9).

 Backpropagate and update ϕ using $\partial L_{\text{RD}}(\phi, \theta) / \partial \phi$, keeping θ fixed.

end for

end for

return Fine-tuned model parameters $\{\phi^*\}$.

Compress $\mathbf{H} \in \mathcal{H}_E$ to latent representation $\bar{\mathbf{Z}} = Q(f_{\phi^*}(\mathbf{H}))$.

Entropy encode: $b_z = \gamma_{\theta_0}(\bar{\mathbf{Z}}; p_{\theta_0})$.

Algorithm 2 Encoder-only Fine-tuning - Decoder

Input: Global decoder model parameters trained on a generic dataset θ_0 , bit stream b_z .

Output: Decompressed CSI matrix $\hat{\mathbf{H}}$.

Apply entropy decoding and de-quantization $\tilde{\mathbf{Z}} = \gamma_{\theta_0}^{-1}(b_z; p_{\theta_0})$, $\bar{\mathbf{Z}} = Q^{-1}(\tilde{\mathbf{Z}})$.

Apply feature decoder network $\hat{\mathbf{H}} = g_{\theta_0}(\bar{\mathbf{Z}})$.

where clipping and rounding operations are defined as:

$$\text{clip}(x, x_{\min}, x_{\max}) = \begin{cases} x_{\min}, & \text{if } x < x_{\min}, \\ x, & \text{if } x_{\min} \leq x \leq x_{\max}, \\ x_{\max}, & \text{if } x > x_{\max}, \end{cases} \quad (13)$$

$$\lfloor x \rfloor = \begin{cases} \lfloor x \rfloor, & \text{if } x - \lfloor x \rfloor < 0.5, \\ \lceil x \rceil, & \text{if } x - \lfloor x \rfloor \geq 0.5. \end{cases} \quad (14)$$

Since both rounding and clipping are non-differentiable operations, they hinder the training of our neural CSI compressor through gradient descent. To address this issue, we employ a common technique called the straight-through estimator (STE) [43], where we approximate $\partial Q_t(\delta) / \partial \delta = 1$. Here, the quantization bin is controlled by t , and N is a hyperparameter that specifies the number of bins. Given that $\bar{\delta} = Q_t(\delta)$, the discrete model prior $p[\bar{\delta}]$ is derived by pushing forward $p(\delta)$ through the quantization function Q_t :

$$\begin{aligned} p[\bar{\delta}] &= \int_{Q_t^{-1}(\bar{\delta})} p(\delta) d\delta \\ &= \int_{\bar{\delta}-t/2}^{\bar{\delta}+t/2} p(\delta) d\delta \\ &= P(\delta < \bar{\delta} + t/2) - P(\delta < \bar{\delta} - t/2). \end{aligned} \quad (15)$$

This means that $p[\bar{\delta}]$ represents the probability mass function of $p(\delta)$ within the bin centered at $\bar{\delta}$. It is computed as the difference between the cumulative density function (CDF) values of $p(\delta)$ at the boundaries of the bin.

After quantization, an appropriate model prior $p(\delta)$ must be carefully selected to enable efficient entropy coding of the discrete model updates. Various distributions can be used to model this prior, such as a Gaussian distribution centered at zero, i.e., $p(\delta) = \mathcal{N}(\mathbf{0}, \sigma^2 \mathbf{I})$. However, a key limitation of the Gaussian prior is its relatively high coding cost for zero-updates. This implies that even when no update is applied, encoding them can still incur a significant bit-rate. To address this inefficiency, we adopt a spike-and-slab prior [44], defined as:

$$p(\delta) = \frac{p_{\text{slab}}(\delta) + \alpha p_{\text{spike}}(\delta)}{1 + \alpha}, \quad (16)$$

where

$$p_{\text{slab}}(\delta) = \mathcal{N}(\delta \mid 0, \sigma^2 \mathbf{I}) \quad (17)$$

is the slab component, and

$$p_{\text{spike}}(\delta) = \mathcal{N}(\delta \mid 0, \frac{t}{6} \mathbf{I}) \quad (18)$$

is the spike component.

Here, $p(\delta)$ is a mixture of Gaussian distributions, where $\alpha \in \mathbb{R}^+$ is a hyperparameter controlling the height of the spike Gaussian relative to the wider slab. The parameters t and σ , with $\sigma \gg t/6$, represent the standard deviations of the spike and slab distributions, respectively. By setting the standard deviation of the spike to $\frac{t}{6}$, nearly 99.7% of its probability mass lies within the central quantization bin after quantization. By selecting a large value of α , the spike component in $p(\delta)$ reduces the bit-rate cost associated with zero-updates and encourages the network to learn only the most informative model updates.

The bit-rate cost for the quantized model updates, $\bar{\delta}$ with prior $p[\bar{\delta}]$ is given by:

$$\bar{M} = -\log_2 p[\bar{\delta}], \quad (19)$$

and can be approximated by its continuous counterpart:

$$M = -\log_2 p(\delta), \quad (20)$$

To regularize the bit-rate cost of model updates during fine-tuning, we include the bit-rate cost of model updates to the RD loss function in Equation 9, specifically:

$$L_{\text{RDM}}(\phi, \theta) = L_{\text{RD}}(\phi, \theta) - \lambda \log_2 p(\delta). \quad (21)$$

By optimizing this loss function during full-model fine-tuning, the network learns to balance the RD gain with the bit-rate cost of model updates.

We summarize the encoding and decoding of the full-model fine-tuning in Algorithms 3 and 4, respectively.

Algorithm 3 Full-model Fine-tuning - Encoding

Input: Global model parameters $\{\theta_0, \phi_0\}$ trained on a generic dataset, batch size B , CSI samples from a new environment $\mathcal{H} = \{\mathcal{H}_{\text{T}}, \mathcal{H}_{\text{E}}\}$.

Output: Compressed bitstream $b = (b_{\bar{\delta}}, b_z)$.

Initialize model parameters: $\phi = \phi_0$, and $\theta = \theta_0$

for epoch = 1 to num_epochs **do**

for each batch b in \mathcal{H}_{T} **do**

 Load data batch $\mathbf{H} \in \{\mathcal{H}_b\}_{b=1}^B$ from \mathcal{H}_{T} .

 Quantize updated decoder parameters: $\bar{\theta} = Q_t(\delta) + \theta_0$, with $\delta = \theta - \theta_0$.

 Apply feature encoder and quantization, $\mathbf{Z} = f_{\phi}(\mathbf{H})$ and $\tilde{\mathbf{Z}} = \mathbf{Z} + \Delta \mathbf{Z}$.

 Apply feature decoder, $\hat{\mathbf{H}} = g_{\theta}(\tilde{\mathbf{Z}})$.

 Compute loss $L_{\text{RDM}}(\phi, \theta)$ according to equation (9).

 Backpropagate using STE for $Q_t(\delta)$, then update θ, ϕ using gradients $\partial L_{\text{RDM}}(\phi, \theta) / \partial \theta$ and $\partial L_{\text{RDM}}(\phi, \theta) / \partial \phi$.

end for

end for

return Fine-tuned model parameters $\{\phi^*, \theta^*\}$.

Compress $\mathbf{H} \in \mathcal{H}_{\text{E}}$ to latent representation $\tilde{\mathbf{Z}} = Q(f_{\phi^*}(\mathbf{H}))$.

Compute quantized model parameters: $\bar{\theta} = \theta_0 + \bar{\delta}$, with $\bar{\delta} = Q_t(\theta^* - \theta_0)$.

Entropy encode: $b_{\bar{\delta}} = \gamma(\bar{\delta}; p[\bar{\delta}])$ and $b_z = \gamma_{\bar{\theta}}(\tilde{\mathbf{Z}}; p_{\bar{\theta}})$.

Algorithm 4 Full-model Fine-tuning - Decoding

Input: Global model parameters θ_0 trained on a generic dataset, model prior $p[\bar{\delta}]$, bitstream $b = (b_z, b_{\bar{\delta}})$.

Output: Decompressed CSI matrix $\hat{\mathbf{H}}$.

Entropy decode: $\bar{\delta} = \gamma^{-1}(b_{\bar{\delta}}; p[\bar{\delta}])$

Compute decoder's updated parameters under model prior: $\bar{\theta} = \theta_0 + \bar{\delta}$

Entropy decode latent under fine-tuned prior: $\tilde{\mathbf{Z}} = \gamma_{\bar{\theta}}^{-1}(b_z; p_{\bar{\theta}})$

Apply de-quantization and feature decoder: $\hat{\mathbf{H}} = Q^{-1}(g_{\bar{\theta}}(\tilde{\mathbf{Z}}))$

IV. PERFORMANCE EVALUATION

In this section, we evaluate the effectiveness of various fine-tuning schemes applied to the backbone model in a new environment with varying channel statistics. We test our fine-tuning approach using the QuaDRiGA and DeepMIMO datasets, as introduced in Section III. Fine-tuning is performed using a small number of CSI samples—specifically, 100 and 127 CSI instances for the QuaDRiGA and DeepMIMO datasets, respectively. For a fair comparison, we use our backbone neural CSI compressor trained with the RDM loss function, instead of the vanilla autoencoder architectures employed in previous works [29]–[35]. It is worth noting that, as demonstrated in [14], neural CSI compression models trained with the RD loss function significantly outperform those that optimize only for distortion. Based on this, both our

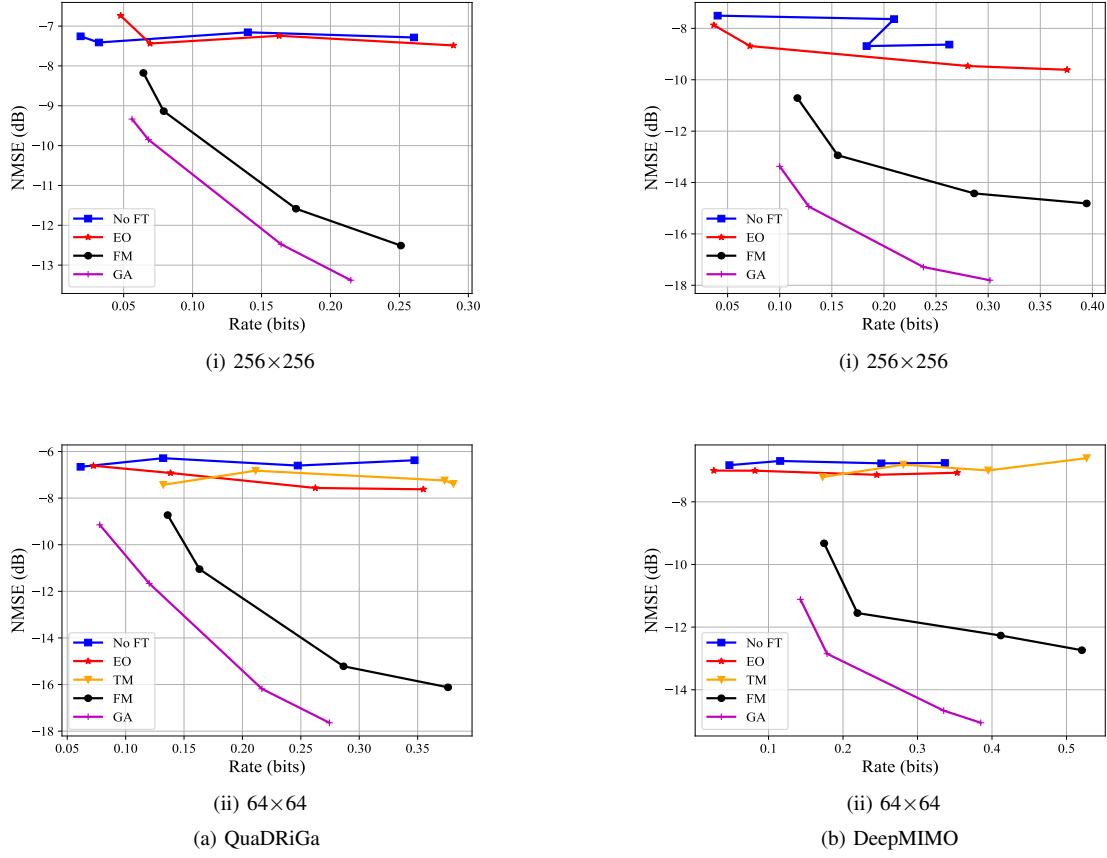


Fig. 7: The RD plot for different fine-tuning schemes, applied to (a) QuaDRiGa and (b) DeepMIMO datasets.

method and prior works can be categorized into the following schemes:

- “No FT” represents applying a pre-trained neural CSI compressor without any fine-tuning in the new environment.
- “EO” shows the results for the encoder-only fine-tuning scheme. We apply fine-tuning to the corresponding trained neural CSI compressor at different λ values. The works in [32], [33], [35] utilized this scheme for their corresponding network.
- “FM” refers to the full-model fine-tuning scheme. We use $t = 0.005$, $N = 50$, $\sigma = 0.05$, and train for 1000 epochs. we only fine-tune the low-bit-rate neural CSI compressor, i.e., the one trained at $\lambda = 5 \times 10^5$ for 256×256 CSI dimension and $\lambda = 5 \times 10^4$, for 64×64 CSI dimension. We emphasize that the reported rate in the plots for this scheme represents the total rate, i.e., the sum of the latent bit-rate and the model update bit-rate. Minor parameter adjustments are made to achieve the best possible performance.
- “GA” represents a ‘genie-aided’ fine-tuning scheme, where we assume that the decoder has perfect knowledge of model updates without any additional feedback overhead. The results for “GA” serve as a lower bound for fine-tuning the neural CSI compressor. Similar to

“FM” fine-tuning, we only use the low-bit-rate trained neural CSI compressor. The work in [29], [32] can be regarded as the “GA” scheme that we have considered in our simulations, they fine-tune a vanilla auto-encoder without accounting for the overhead required for model update feedback.

- “TM” refers to the ‘translation module’ introduced in [30]. This scheme, inspired by image-to-image translation in computer vision, adapts the input data to a new domain by utilizing the translation module. Specifically, convolutional translation and retranslation modules are applied at the encoder and decoder, respectively. We use the same network architecture and sparsity-aligning function for translation/retranslation modules as in [30]. Similar to “EO” fine-tuning, we use neural CSI compressors trained at different λ . Furthermore, we ignore the communication overhead for feedbacking the retranslation module’s parameters to the decoder side to provide the lower bound rate throughout the simulation for this scheme.

To the best of our knowledge, we have included all major benchmarks for CSI compression fine-tuning in our simulations, except for [31]. The work in [31] relies on a finite number of datasets and decoder models, making a fair comparison in our simulation setup impossible. We present a comparison of the aforementioned fine-tuning schemes in Fig. 7 for the

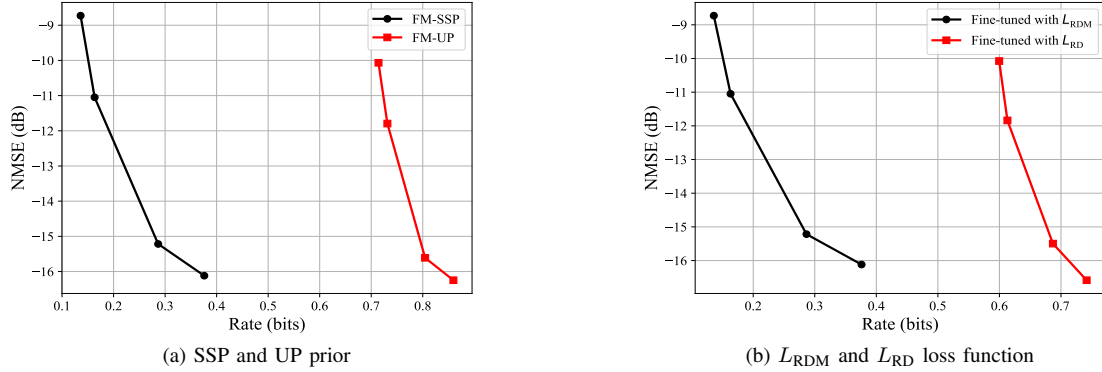


Fig. 8: The effect of spike-and-slap prior and L_{RDM} loss function on the RD performance of full-model fine-tuning.

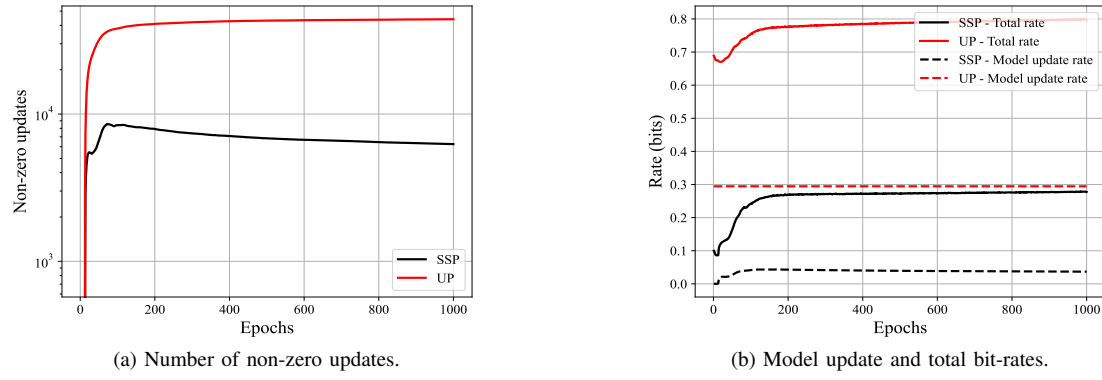


Fig. 9: Number of non-zero model updates and update bit-rates using spike-and-slab and uniform priors.

QuaDRiGa and DeepMIMO datasets. The reported bit-rate in all the following plots is normalized with respect to the CSI dimensions, i.e., $N_t \times N_c$. A learning rate of 0.0001 is used for all simulations. The fine-tuning scheme in [30] is excluded for the 256×256 CSI dimension due to its extreme computational complexity, as the translation module employs a brute-force algorithm in its sparsity-aligning function. The results indicate that the ‘‘EO’’ and ‘‘TM’’ fine-tuning schemes provide only marginal improvements in RD performance. This suggests that modifying only the encoder or applying domain adaptation techniques is insufficient to fully adapt the model to new CSI statistics. In contrast, the ‘‘FM’’ fine-tuning approach achieves a significant RD performance boost. This finding underscores the importance of end-to-end fine-tuning of the entire model.

To examine the impact of L_{RDM} loss function and the spike-and-slab prior on full-model fine-tuning, Fig. 8 presents an ablation study on the QuaDRiGa dataset for CSI dimensions of 64×64 . Fig. 8a shows the results when a different prior distribution, e.g., uniform, is used for model updates, while Fig. 8b presents the RD performance when regularization of the model updates is excluded from the loss function, i.e., trained with L_{RD} (with spike-and-slab prior). ‘FM-SSP’ refers to spike-and-slab prior, while ‘FM-UP’ represents a uniform prior assumed for entropy coding of model updates.

The RD results in these figures highlight the importance of both the spike-and-slab prior and the regularization of the model updates in L_{RDM} for the full-model fine-tuning scheme. Using a uniform prior or omitting regularization of the model updates causes the model update rate to explode during fine-tuning, resulting in an extremely high bit-rate. In contrast, incorporating both the spike-and-slab prior and fine-tuning with L_{RDM} helps maintain low and effective model update costs.

To elaborate on how the spike-and-slab prior reduces the bit-rate of model updates, Fig. 9 presents the number of non-zero updates during fine-tuning, along with the bit-rate of model updates and the total bit-rate. These are compared against the uniform prior baseline. As shown in the figure, the spike-and-slab prior results in significantly fewer non-zero model updates, thereby substantially reducing the bit-rate of model updates and, consequently, the total bit-rate. The spike component of the prior enforces sparsity in the model updates by selecting only the most impactful parameters that contribute to the RD loss function.

In Table IV, the RD performance of full-model fine-tuning is reported for different quantization resolutions evaluated on the QuaDRiGa dataset for CSI dimension of 64×64 . In each RD pair, the first value represents the normalized bit-

TABLE IV: The impact of quantization resolution of model updates on RD.

Quantization	RD
2-bit	(0.34, -5.08)
4-bit	(0.39, -7.33)
8-bit	(0.38, -11.25)
16-bit	(0.35, -14.55)
32-bit	(0.31, -15.24)
64-bit	(0.28, -15.35)
128-bit	(0.28, -15.15)
256-bit	(0.28, -15.06)

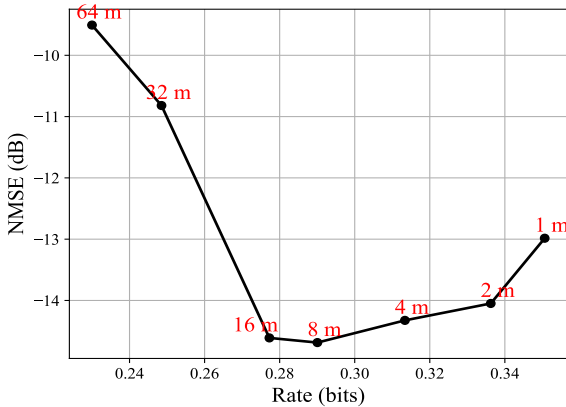


Fig. 10: Full-model RD performance across varying distances for the mobile user in the QuaDRiGa dataset.

rate, and the second denotes the NMSE (in dB). Comparing the RD pairs across various quantization bit levels shows that 64-bit quantization achieves the best RD trade-off. Using lower-resolution quantization (≤ 8 bits) leads to significant performance degradation, while higher-resolution quantization (≥ 128 bits) does not yield any noticeable RD improvement.

We note again that encoder-only fine-tuning can be applied for each channel realization as it does not impose any additional cost on the rate. However, any update to the decoder network must be communicated to the decoder. Therefore, it might be better to update the decoder network only at certain times when the CSI statistics change noticeably. Accordingly, for full-model fine-tuning, we consider the duration over which the fine-tuning scheme is applied. If fine-tuning is applied over a longer period, the additional bit-rate required for model updates will decrease, albeit at the cost of increased mismatch between the statistics of the CSI samples used for inference and fine-tuning. Conversely, shorter fine-tuning periods lead to higher bit-rates for model updates, but the channel statistics will be more similar to the CSI realizations used to fine-tune the entire model, which will result in better distortion efficiency. Thus, there is a trade-off in determining how often fine-tuning and updating the decoder's parameters need to be applied.

To explore this trade-off, we apply full-model fine-tuning across varying distances for the mobile user in the QuaDRiGa

TABLE V: Number of FLOPs, trainable parameters, and Big-O analysis for different fine-tuning schemes M: million, K: thousand.

	Parameters	FLOPs	Big-O
EO	109 K	475 M	$\mathcal{O}(N_t N_c)$
FM	218 K	475 M	$\mathcal{O}(N_t N_c)$
TM	8 K	521 M	$\mathcal{O}(N_t N_c)$

dataset. The RD plot for this simulation is shown in Fig. 10, with RD weight $\lambda = 5 \times 10^5$ for 64×64 CSI dimensions. From Fig. 10, we observe that the optimal distance for performing full-model fine-tuning, in terms of RD performance, lies approximately between 8 and 16 meters. Updating the model more frequently than every 8 meters incurs a high cost for model update bits. On the other hand, updating the model less frequently than every 16 meters, while reducing the bit-rate cost, leads to increased channel variation that negatively impacts the RD performance. Thus, operators must choose to fine-tune the model at a certain frequency to enhance compression efficiency. This period should depend on the CSI statistics and the backbone CSI compressor; for different CSI environments and network architectures, the optimal period will vary.

Table V compares the Big-O complexity, the number of floating-point operations (FLOPs) required during inference, and the number of trainable parameters for different fine-tuning schemes. The computational cost of fine-tuning depends on the complexity of the backbone neural compressor and the CSI dimensions. The results in Table V reflect the computational complexity when using the backbone neural compressor shown in Fig. 1 with 64×64 CSI dimensions. As the table shows, our backbone network exhibits moderate complexity compared to many architectures in the literature, requiring approximately 475 FLOPs during inference. For comparison, the authors of [30] employed SPTM2-ISTANet+, which unfolds an iterative shrinkage-thresholding algorithm and requires significantly more computation—approximately 25.5 billion FLOPs for 12 iterations. For a fixed neural network architecture, the Big-O complexity of a CNN scales with the input CSI dimensions, meaning larger CSI matrices will lead to higher computational cost. In the encoder-only fine-tuning scheme—where the decoder and latent parameters are fixed—the number of trainable parameters is less than half that of full-model fine-tuning. When translation modules are used while keeping the backbone compressor fixed, the number of trainable parameters scales solely with the parameters of the translation modules. As illustrated in Fig. 7, any fine-tuning scheme that does not jointly update both the encoder and decoder of the backbone model leads to only marginal improvements in RD performance.

V. CONCLUSION

A major limitation of neural compression approaches is their drastic performance degradation when channel statistics change, a natural phenomenon in wireless environments. To address this distribution shift problem, we proposed a

model fine-tuning scheme for neural CSI compression. In this scheme, the encoder, having access to the most recent CSI samples, fine-tunes both the encoder and decoder models to enhance compression efficiency under varying CSI statistics. While the encoder can directly use the fine-tuned model at no additional cost, the updated model must be communicated to the decoder, introducing an extra model update cost to the compression rate, which has been neglected in all previous works that involved fine-tuning neural CSI compression models. We employed lossless entropy coding for both latent and model updates and adopted a spike-and-slap prior distribution to promote sparse and efficient parameter updates. Additionally, we incorporated the bit-rate of model updates into the fine-tuning process by using a regularized RD loss function.

Simulation results demonstrated that the proposed full-model fine-tuning approach is essential for adapting the neural CSI compressor to varying environments. Furthermore, we revealed the significance of using the spike-and-slap prior to reduce the excessive bit-rate cost of model updates. Since model updates introduce additional overhead to the communication rate, we also analyzed how frequently the fine-tuning scheme should be applied, highlighting the trade-offs between using this approach over short and long periods of new CSI realizations. Our results reveal a sweet spot for the frequency of model updates, which depends on the environment, network architecture, and mobility pattern of the user. This work can be extended to adaptive fine-tuning of neural CSI compressors in scenarios with high-mobility users, which we will explore as a future direction. In such scenarios, the encoder could judiciously decide when to fine-tune and update the model parameters based on variations in CSI statistics, rather than adhering to a fixed update frequency.

REFERENCES

- [1] T. L. Marzetta, “Noncooperative cellular wireless with unlimited numbers of base station antennas,” *IEEE Trans. Wireless Commun.*, vol. 9, no. 11, pp. 3590–3600, 2010.
- [2] E. G. Larsson, O. Edfors, F. Tufvesson, and T. L. Marzetta, “Massive MIMO for next generation wireless systems,” *IEEE Commun. Mag.*, vol. 52, no. 2, pp. 186–195, 2014.
- [3] X. Rao and V. K. N. Lau, “Distributed compressive CSIT estimation and feedback for FDD multi-user massive MIMO systems,” *IEEE Trans. Signal Process.*, vol. 62, no. 12, pp. 3261–3271, 2014.
- [4] X.-L. Huang, J. Wu, Y. Wen, F. Hu, Y. Wang, and T. Jiang, “Rate-adaptive feedback with bayesian compressive sensing in multiuser MIMO beamforming systems,” *IEEE Trans. Wireless Commun.*, vol. 15, no. 7, pp. 4839–4851, 2016.
- [5] V. Rizzello, M. Nerini, M. Joham, B. Clerckx, and W. Utschick, “User-driven adaptive CSI feedback with ordered vector quantization,” *IEEE Wireless Commun. Lett.*, vol. 12, no. 11, pp. 1956–1960, 2023.
- [6] R. Bhagavatula and R. W. Heath, “Predictive vector quantization for multicell cooperation with delayed limited feedback,” *IEEE Trans. Wireless Commun.*, vol. 12, no. 6, pp. 2588–2597, 2013.
- [7] C. Wen, W. Shih, and S. Jin, “Deep learning for massive MIMO CSI feedback,” *IEEE Wireless Commun. Lett.*, vol. 7, no. 5, pp. 748–751, Mar. 2018.
- [8] J. Guo, C.-K. Wen, S. Jin, and G. Y. Li, “Convolutional neural network-based multiple-rate compressive sensing for massive MIMO CSI feedback: Design, simulation, and analysis,” *IEEE Trans. Wireless Commun.*, vol. 19, no. 4, pp. 2827–2840, 2020.
- [9] Z. Lu, J. Wang, and J. Song, “Multi-resolution CSI feedback with deep learning in massive MIMO system,” in *Proc. IEEE Int. Conf. Commun. (ICC)*, 2020, pp. 1–6.
- [10] S. Tang, J. Xia, L. Fan, X. Lei, W. Xu, and A. Nallanathan, “Dilated convolution based CSI feedback compression for massive MIMO systems,” *IEEE Trans. Veh. Technol.*, vol. 71, no. 10, pp. 11216–11221, 2022.
- [11] Y. Cui, A. Guo, and C. Song, “Transnet: Full attention network for CSI feedback in FDD massive MIMO system,” *IEEE Wireless Commun. Lett.*, vol. 11, no. 5, pp. 903–907, 2022.
- [12] Z. Hu, G. Liu, Q. Xie, J. Xue, D. Meng, and D. Gündüz, “A learnable optimization and regularization approach to massive MIMO CSI feedback,” *IEEE Trans. Wireless Commun.*, vol. 23, no. 1, pp. 104–116, 2024.
- [13] H. Wu, M. Zhang, Y. Shao, K. Mikolajczyk, and D. Gündüz, “MIMO channel as a neural function: Implicit neural representations for extreme CSI compression in massive MIMO systems,” 2024. [Online]. Available: <https://arxiv.org/abs/2403.13615>
- [14] M. B. Mashhadi, Q. Yang, and D. Gündüz, “Distributed deep convolutional compression for massive MIMO CSI feedback,” *IEEE Trans. Wireless Commun.*, vol. 20, no. 4, pp. 2621–2633, 2021.
- [15] W. Chen, W. Wan, S. Wang, P. Sun, G. Y. Li, and B. Ai, “CSI-PPPNet: A one-sided one-for-all deep learning framework for massive MIMO CSI feedback,” 2023. [Online]. Available: <https://arxiv.org/abs/2211.15851>
- [16] Y. Yang, S. Mandt, and L. Theis, “An introduction to neural data compression,” *Found. Trends. Comput. Graph. Vis.*, vol. 15, no. 2, p. 113–200, apr 2023. [Online]. Available: <https://doi.org/10.1561/0600000107>
- [17] I. Goodfellow, J. Pouget-Abadie, M. Mirza, B. Xu, D. Warde-Farley, S. Ozair, A. Courville, and Y. Bengio, “Generative adversarial nets,” in *Adv. Neural Inf. Process. Syst.*, Z. Ghahramani, M. Welling, C. Cortes, N. Lawrence, and K. Weinberger, Eds., vol. 27. Curran Associates, Inc., 2014. [Online]. Available: https://proceedings.neurips.cc/paper_files/paper/2014/file/5ca3e9b122f61f8f06494c97b1a7ccf3-Paper.pdf
- [18] D. P. Kingma and M. Welling, “Auto-Encoding Variational Bayes,” in *2nd Int. Conf. Learn. Represent. (ICLR) 2014, Banff, AB, Canada, Apr. 14–16, 2014, Conf. Track Proc.*, 2014.
- [19] H. Larochelle and I. Murray, “The neural autoregressive distribution estimator,” in *Proc. 14th Int. Conf. Artif. Intell. Stat. (AISTATS)*, ser. Proc. Mach. Learn. Res., G. Gordon, D. Dunson, and M. Dudík, Eds., vol. 15. Fort Lauderdale, FL, USA: PMLR, 11–13 Apr 2011, pp. 29–37. [Online]. Available: <https://proceedings.mlr.press/v15/larochelle11a.html>
- [20] A. van den Oord, N. Kalchbrenner, and K. Kavukcuoglu, “Pixel recurrent neural networks,” in *Proc. 33rd Int. Conf. Mach. Learn. (ICML)*, ser. Proc. Mach. Learn. Res., M. F. Balcan and K. Q. Weinberger, Eds., vol. 48. New York, NY, USA: PMLR, 20–22 Jun 2016, pp. 1747–1756. [Online]. Available: <https://proceedings.mlr.press/v48/oord16.html>
- [21] Q. Yang, M. B. Mashhadi, and D. Gündüz, “Deep convolutional compression for massive MIMO CSI feedback,” in *Proc. IEEE 29th Int. Workshop Mach. Learn. Signal Process. (MLSP)*, 2019, pp. 1–6.
- [22] J. Quiñonero-Candela, M. Sugiyama, A. Schwaighofer, and N. D. Lawrence, *Dataset Shift in Machine Learning*. MIT Press, 2022.
- [23] F. Zhuang, Z. Qi, K. Duan, D. Xi, Y. Zhu, H. Zhu, H. Xiong, and Q. He, “A comprehensive survey on transfer learning,” *Proc. IEEE*, vol. 109, no. 1, pp. 43–76, 2020.
- [24] R. Volpi, H. Namkoong, O. Sener, J. C. Duchi, V. Murino, and S. Savarese, “Generalizing to unseen domains via adversarial data augmentation,” in *Adv. Neural Inf. Process. Syst. (NeurIPS)*, S. Bengio, H. Wallach, H. Larochelle, K. Grauman, N. Cesa-Bianchi, and R. Garnett, Eds., vol. 31. Curran Associates, Inc., 2018. [Online]. Available: https://proceedings.neurips.cc/paper_files/paper/2018/file/1d94108e907bb8311d8802b48fd54b4a-Paper.pdf
- [25] Y. Ganin and V. Lempitsky, “Unsupervised domain adaptation by backpropagation,” in *Int. Conf. Mach. Learn. (ICML)*. PMLR, 2015, pp. 1180–1189.
- [26] M. Sattari, H. Guo, D. Gündüz, A. Panahi, and T. Svensson, “Full-duplex millimeter wave MIMO channel estimation: A neural network approach,” *IEEE Trans. Mach. Learn. Commun. Netw.*, vol. 2, pp. 1093–1108, 2024.
- [27] M. Khani, M. Alizadeh, J. Hoydis, and P. Fleming, “Adaptive neural signal detection for massive MIMO,” *IEEE Trans. Wirel. Commun.*, vol. 19, no. 8, pp. 5635–5648, May. 2020.
- [28] M. Jankowski, D. Gündüz, and K. Mikolajczyk, “Airnet: Neural network transmission over the air,” in *2022 IEEE Int. Symp. Inf. Theory (ISIT)*, 2022, pp. 2451–2456.
- [29] J. Zeng, J. Sun, G. Gui, B. Adebisi, T. Ohtsuki, H. Gacanin, and H. Sari, “Downlink CSI feedback algorithm with deep transfer learning for FDD massive MIMO systems,” *IEEE Trans. Cogn. Commun. Netw.*, vol. 7, no. 4, pp. 1253–1265, 2021.

[30] Z. Liu, L. Wang, L. Xu, and Z. Ding, “Deep learning for efficient CSI feedback in massive MIMO: Adapting to new environments and small datasets,” *IEEE Trans. Wireless Commun.*, pp. 1–1, 2024.

[31] X. Li, J. Guo, C.-K. Wen, S. Jin, S. Han, and X. Wang, “Multi-task learning-based CSI feedback design in multiple scenarios,” *IEEE Trans. Commun.*, vol. 71, no. 12, pp. 7039–7055, 2023.

[32] B. Zhang, H. Li, X. Liang, X. Gu, and L. Zhang, “Model transmission-based online updating approach for massive mimo csi feedback,” *IEEE Communications Letters*, vol. 27, no. 6, pp. 1609–1613, 2023.

[33] X. Zhang, J. Wang, Z. Lu, and H. Zhang, “Continuous online learning-based csi feedback in massive mimo systems,” *IEEE Communications Letters*, vol. 28, no. 3, pp. 557–561, 2024.

[34] Y. Cui, J. Guo, C.-K. Wen, and S. Jin, “Communication-efficient personalized federated edge learning for massive mimo csi feedback,” *IEEE Transactions on Wireless Communications*, vol. 23, no. 7, pp. 7362–7375, 2024.

[35] J. Guo, Y. Zuo, C.-K. Wen, and S. Jin, “User-centric online gossip training for autoencoder-based csi feedback,” *IEEE Journal of Selected Topics in Signal Processing*, vol. 16, no. 3, pp. 559–572, 2022.

[36] L. Theis and E. Agustsson, “On the advantages of stochastic encoders,” *CoRR*, vol. abs/2102.09270, 2021. [Online]. Available: <https://arxiv.org/abs/2102.09270>

[37] Y. Yang and S. Mandt, “Towards empirical sandwich bounds on the rate-distortion function,” *ArXiv*, vol. abs/2111.12166, 2021. [Online]. Available: <https://api.semanticscholar.org/CorpusID:244527239>

[38] J. Ballé, D. Minnen, S. Singh, S. J. Hwang, and N. Johnston, “Variational image compression with a scale hyperprior,” in *Int. Conf. Learn. Represent. (ICLR)*, 2018. [Online]. Available: <https://openreview.net/forum?id=rkcQFMZRb>

[39] Remcom, “Wireless InSite,” <http://www.remcom.com/wireless-insite>.

[40] S. Jaeckel, L. Raschkowski, K. Börner, and L. Thiele, “Quadriga: A 3-d multi-cell channel model with time evolution for enabling virtual field trials,” *IEEE Trans. Antennas Propag.*, vol. 62, no. 6, pp. 3242–3256, 2014.

[41] A. Alkhateeb, “DeepMIMO: A generic deep learning dataset for millimeter wave and massive MIMO applications,” in *Proc. Inf. Theory Appl. Workshop (ITA)*, San Diego, CA, Feb 2019, pp. 1–8.

[42] T. van Rozendaal, I. A. Huijben, and T. Cohen, “Overfitting for fun and profit: Instance-adaptive data compression,” in *Int. Conf. Learn. Represent. (ICLR)*, 2021. [Online]. Available: https://openreview.net/forum?id=oFp8Mx_V5FL

[43] Y. Bengio, N. Léonard, and A. C. Courville, “Estimating or propagating gradients through stochastic neurons for conditional computation,” *CoRR*, vol. abs/1308.3432, 2013, accessed: 2025-01-27. [Online]. Available: <http://arxiv.org/abs/1308.3432>

[44] V. Ročková and E. I. G. and, “The spike-and-slab lasso,” *Journal of the American Statistical Association*, vol. 113, no. 521, pp. 431–444, 2018. [Online]. Available: <https://doi.org/10.1080/01621459.2016.1260469>